Published in final edited form as:
Cancer. 2012 November 15; 118(22): 5698–5708. doi:10.1002/cncr.27629.

IL13Rα2 is a novel therapeutic target for human adrenocortical carcinoma

Meenu Jain[1], **Lisa Zhang**[1], **Mei He**[1], **Erin E. Patterson**[1], **Naris Nilubol**[1], **Antonio T. Fojo**[3], **Bharat Joshi**[2], **Raj Puri**[2], and **Electron Kebebew**[1]

[1]Endocrine Oncology Section, Surgery Branch, National Cancer Institute, National Institute of Health, Bethesda, Maryland 20892

[2]Tumor Vaccines and Biotechnology Branch, Division of Cellular and Gene Therapies, Center for Biologics Evaluation and Research, Food and Drug Administration, Bethesda, Maryland 20892

[3]Medical Oncology Branch, National Cancer Institute, National Institute of Health, Bethesda, Maryland 20892

Abstract

Background—Adrenocortical carcinoma (ACC) is a relatively rare but aggressive malignancy with limited therapeutic options. Previous genome wide expression studies have shown overexpression of Interleukin-13 receptor alpha2 (*IL13Rα2*) in some human malignancies.

Methods—We evaluated IL13Rα2 mRNA and protein expression in 21 normal, 78 benign, 10 primary malignant, and 25 metastatic/recurrent samples, and performed functional with IL13 ligand and *IL13 Rα2* knockdown in vitro. We evaluated the sensitivity of two ACC cell lines (NCI-H295R-high IL13Rα2 expression, SW13- low IL13Rα2 expression) to a highly specific IL-13 targeting immunotoxin (IL-13 conjugated with pseudomonas exotoxin, IL-13-PE) in *in vitro* and *in vivo*.

Results—IL13Rα2 was overexpressed in malignant tumors compared to benign and normal (15-fold higher, $p<0.05$). Immunohistochemistry also confirmed higher protein expression in malignant and benign tumors than normal adrenocortical tissues ($p<0.05$). We found the half-maximal inhibitory concentration for IL-13-PE was 1.3 ng/ml (NCI-H295R) and 1000 ng/ml (SW13) in the cell lines. Mice receiving intratumoral or intraperitoneal IL-13-PE injection showed a significant reduction in tumor size and tumor necrosis compared to control groups ($p<0.05$) and prolonged survival ($p<0.05$). IL13Rα2 protein expression increased in cells treated with IL-13 ligand, as well as, cell invasion ($p < 0.05$). Direct *IL13Rα2* knockdown decreased cellular proliferation and invasion ($p < 0.05$).

Conclusions—Our study results indicate that *IL13Rα2* is overexpressed in ACC and regulates cell invasion and proliferation. *IL13Rα2* is a novel therapeutic target for the treatment of human ACC.

Keywords

IL13Rα2; IL-13-PE; adrenocortical carcinoma; invasion

Corresponding author: Electron Kebebew MD, Endocrine Oncology Section, Surgery Branch, National Cancer Institute, 10-CRC - Hatfield Clinical Research Center, 4-5952, Bethesda, MD, Zip Code 20892, Telephone: 301-496-5049, Fax: 301- 402-1788, electron.kebebew@nih.gov.

Introduction

With an annual incidence of approximately 0.72 cases per million, adrenocortical carcinoma (ACC) is a rare malignancy of the adrenal cortex with poorly understood mechanism of development [1; 2; 3; 4]. Currently, surgical resection is the only possible curative therapy for ACC but since the majority of patients present with metastatic disease, the five-year survival rate is less than 10% [1; 5]. Therefore, there is a significant need for new therapeutic options that may be effective in patients with ACC.

Since the molecular mechanism of adrenocortical tumorigenesis is not clearly defined, genome wide gene expression profiling analysis of adrenocortical tumors has been used to determine dysregulated gene expression associated with ACC [6; 7; 8; 9; 10; 11]. Interleukin-13 receptor alpha2 (*IL13Rα2*) was one gene that was found to be overexpressed in ACC [10]. IL13Rα2 is a high-affinity receptor of Th2-derived cytokine interleukin-13 (IL-13), and is overexpressed in several tumors as compared to low or absent expression in normal cells and tissues [12; 13; 14; 15; 16; 17; 18]. Initial studies suggested that IL13Rα2 binds IL-13 ligand with high affinity but without activating any signal transduction pathways [19]. Therefore, it was hypothesized that the function of the extracellular domain of IL13Rα2 was to serve as a decoy receptor to regulate the signaling of type II IL-13R complex (IL-13, *IL13Rα1* and *IL-4α*) through the JAK-STAT6 pathway [20; 21]. However, recently, it has been demonstrated that high affinity binding of IL-13 ligand to IL13Rα2 does signal through a STAT-6 independent AP-1 pathway, which leads to increased TGF-β activity [22].

Targeting cell-surface receptors or antigens with small molecules or immunotoxin therapies is an attractive strategy for development of effective cancer therapy [23; 24]. It has been shown that a chimeric fusion protein that consists of IL-13 and a mutated form of *Pseudomonas* exotoxin (IL-13-PE) is highly cytotoxic to IL13Rα2 positive cancer cells in *in vitro* and *in vivo* models of several malignancies [15; 25; 26].

The present study shows that *IL13Rα2* is overexpressed in ACC. Furthermore, *IL13Rα2* influences ACC cell invasion and is a good therapeutic target in ACC cells in both *in vitro* and *in vivo* models using IL-13-PE immunotoxin.

Materials and Methods

Tissue specimens

Our Institutional Review Board approved the protocol and all material was collected after written informed consent was obtained from patients. Adrenal tissues were snap frozen at the time of surgery and stored at −80°C. IL13Rα2 mRNA and protein expression were determined in 134 human adrenocortical tissue specimens (21 normal, 78 benign adrenocortical tumors, 10 primary ACC, 23 ACC metastases, 2 ACC recurrences). The diagnosis of unequivocal ACC was confirmed in all cases by histologic examination, the presence of lymph nodes metastasis, distant metastasis and or development of locoregional recurrent disease during follow up.

Cell culture and reagents

The NCI-H295R and SW13 ACC cell lines (ATCC, Rockville, MD) were grown and maintained in DMEM supplemented with 1% Insulin Transferrrin Selenium (ITS) (BD Biosciences, San Jose, CA) and 2.5% Nu-Serum I (BD Biosciences) in a standard humidified incubator at 37°C in a 5% CO_2 atmosphere. PM-RCC, a renal cell carcinoma cell line, was maintained in DMEM with 10% fetal bovine serum (Bio-Whittaker Inc., Walkersville, MD), 1 mm HEPES, 1 mm nonessential amino acids, 100 μg/ml penicillin,

and 100 μg/ml streptomycin (Bio-Whittaker Inc.). The recombinant IL-13-PE used in our studies has been described previously [25; 27]. IL-13 was obtained from Sigma (Sigma, St. Louis, MO).

Immunohistochemical (IHC) and Immunocytochemical staining

Sections were deparaffinized, rehydrated and incubated with the primary anti-*IL13Rα2* goat polyclonal antibody (R&D Systems; AF146) at 15 μg/ml dilution overnight at 4°C followed by biotinylated secondary antibody (1:200; Vector Laboratories, Burlingame, CA) for 1 hour at room temperature. Sections were developed using 3,3′-diaminobenzidine DAB as the chromogen (ABC elite kit, Vector Laboratories, CA, USA) and counterstained with hematoxylin. The slides were scanned under an Olympus light microscope (Nikon, Tokyo, Japan) and images were acquired at 20X and 40X magnifications. A semiquantitative scoring system was used to analyze IL13Rα2 expression; expression level was classified as no staining (0), <30% cell staining (1), 30–50% cell staining (2) and >50% cell staining (3). Two observers, who were blinded to the tumor type, independently scored each sample.

Immunofluoroscence staining was done using cultured NCI-H295R cells (1×10^5 in 1 ml) on chamber slides (Lab-Tek, Rochester, NY). Cells were allowed to adhere to slides for 48 hours and incubated with IL-13 at 50 ng/ml for another 48 hours. Cells were washed with PBS and fixed with 4% formaldehyde for 30 minutes. The cells were incubated with primary anti-*IL13Rα2* goat polyclonal antibody at 1:100 dilution overnight (R&D; AF146) at 4°C. The primary antibodies were detected with fluorophore conjugated with RedTX anti-goat IgG (Invitrogen, Carlsbad, CA). The slides were then rinsed and mounted with DAPI (4′, 6-diamidino-2-phenylindole) mounting solution. Images were captured with a Zeiss Axioskop-2 microscope at 20X and 40X magnifications.

Reverse transcription and real time quantitative PCR

RNA samples from tissue samples and cell lines were subjected to RT-PCR analysis. Total RNA (200–500 ng) was reverse-transcribed using a High Capacity Reverse Transcription cDNA kits according to the manufacturer's instructions (Applied Biosystems, Foster City, CA). Real time quantitative PCR was used to measure mRNA expression levels and glyceraldehyde-3-phosphate dehydrogenase (GAPDH) mRNA amplification from the same samples served as an internal control. Normalized gene expression level was represented as $2^{\wedge-}$(Ct of gene of interest $^-$ Ct of GAPDH) × 100%, where Ct is the PCR cycle threshold. The PCR primers probes for *IL13Rα2* (Hs_010180383_m1) and *GAPDH* (Hs99999905_m1) were obtained from Applied Biosystems (Applied Biosystems, Foster City, CA). All reactions were performed in a final volume of 10 μl with 2 μl of cDNA template on a 7900HT Fast Real-Time PCR System (Applied Biosystems, Foster City, CA). The thermal cycler condition was 95°C for 12 minutes followed by 40 cycles of 95°C for 15 seconds and 60°C for 1 minute.

Cell culture and transient transfection

Cells were seeded in 24 and 6 well plates (4×10^4 cells in 0.5 ml and 1.6×10^5 cells in 2 ml, respectively). Twenty-four hours after plating, cells were transfected with either a nonspecific negative control siRNA (AM4613) or a combination of *IL13Rα2* specific siRNAs at a final concentration of 80 nM (s7376 and s7374, Applied Biosystems, Foster City, CA). The TransIT-siQuest reagent (Mirus Bio LLC, Madison, WI) was used to deliver siRNA to the cells according to the manufacturer's instructions.

Cell proliferation

Cells were plated at a concentration of 5×10^3 cells per 100 μL culture medium in a 96-well plate in six replicates. Cell number was determined by using the CyQUANT™ assay kit (Invitrogen, Carlsbad, CA) and a fluorometric microplate reader (Molecular Devices, Sunnyvale, CA) at 480 nm/520 nm.

Flow cytometry

Seven days after transfection, cells (1×10^5) were incubated with 5 μg/mL of mouse monoclonal anti-*IL13Rα2* (Diaclone; B-D13; Rockland, Gilbertsville, PA). The positive staining or binding in the cells was detected using secondary goat anti-mouse IgG conjugated with FITC (Sigma-Aldrich, St. Louis, MO). The fluorescence associated with the live cells was measured using FACS Calibur (BD Biosciences). The cells were gated using secondary FITC conjugated antibody control.

Cell invasion assay

The extent of cell invasion was assessed using the BD BioCoat™ Matrigel™ Invasion Chamber (BD Biosciences, Bedford, MA) according to the manufacturer's protocol. A total of 1×10^5 cells were seeded onto the inserts (8-μM pore sized polycarbonate membrane) coated with a thin layer of Matrigel Basement Membrane Matrix (BD Biosciences). The inserts were placed into a 24-well plate with 10% serum-containing culture medium as chemoattractant. The plates were incubated for 48 hours at 37 °C. Cells that invaded the Matrigel matrix to the lower surface of the membrane were fixed and stained with Diff Quik Stain (Dade Behring, Newark, USA) and counted under a light microscope.

Protein synthesis inhibition assay

A total of 1×10^4 cells were plated in 96-well plate in 100 μl of complete growth medium for 24 hrs. After 24 hrs, the plates were replaced with leucine-free medium (Biofluids, Rockville, MD) for 6 hours. IL-13-PE immunotoxin was added to the cells at 0.1–1000 ng/ml and incubated for 20 hours at 37°C. One μCi of [^{3}H] labeled leucine (NEN Research Products, Boston, MA) was then added to each well, and incubated for an additional 4 hours. Cells were harvested and labeled leucine incorporation was measured by a β plate counter (Perkin Elmer, Waltham, MA). The half-maximal inhibitory concentration (IC_{50}) was defined as the concentration of a drug where the proliferation was reduced by 50%.

Protein synthesis inhibition assay was performed on day 3 after *IL13Rα2* siRNA and negative control transfection. The transfection was carried out with final concentration of 100 nM of *IL13Rα2* siRNA and negative control using 0.2 μl/well of TransIT-siQUEST Transfection Reagent. After 48 hours, the cells were treated with different concentration of IL-13-PE immunotoxin to assess the biological activity of silenced *IL13Rα2*. The IC_{50} values of the silenced cells were compared with negative control and medium. The experiment was performed in quadruplicate with two independent biological repeats.

Tumor spheroids

A total of 1×10^5 NCI-H295R cells/well (in 0.5 ml) were plated in 24-well Ultra low cluster plate (Costar, Corning, NY) to generate tumor spheroids. The plates were cultured at 37°C in 5% CO_2 for one week and the medium was changed every 3 days. After one week of culture, tumor spheroids were photographed under dissecting microscope and were treated with the different concentrations (0.13– 6.5 ng/ml) of IL-13-PE or vehicle (0.2% human serum albumin in PBS) in duplicates. The tumor spheroids were treated for two weeks (dosed every first and third day).

ACC xenografts in athymic nude mice

The institutional animal care and use committee (ACUC) approved the ACC xenograft animal study protocol. Five to six weeks old (body weight, 20–22g) female athymic NCr nu/nu mice were obtained from Frederick Cancer Center Animal Facilities (National Cancer Institute, Frederick, MD). The mice were maintained according to the guidelines of the institute animal advisory committee. NCI-H295R cells were implanted by subcutaneous injection on the left flank with 4×10^6 cells in 100 μl of DMEM and matrigel (1:1). The tumor sizes were measured every 7 days and recorded in mm^3 (length × $width^2/2$). For tumor therapy experiments, the mice were grouped into five groups with six mice per group. Group I and II mice were intratumorally (IT) injected (using Hamilton syringes-80400-22s/2 inch) with 25 μl of IL-13-PE (100 μg/kg) every other day for 1 and 2 weeks, respectively. Group III mice received intraperitoneal (IP) injection (using 27 gauge needle) of 50 μl of IL-13-PE (50 μg/kg) every other day for 1 week. Group IV and V mice received 0.2% human serum albumin (vehicle) every other day for 2 week by IT and IP routes, respectively. Mice were followed until the protocol end point (when the tumor reached size of ≥2cm) and euthanized for further investigations. Tumors and vital organs such as liver, kidney, spleen and lung were removed and fixed in 10% formalin for histopathology examinations.

Statistical Analyses

Continuous data is represented as mean ± standard deviation (S.D.). Two-tailed ANOVA multi-comparison *t*-test was used to assess the difference among normal, benign and malignant samples. A *p*-value <0.05 was considered as significant. The statistical analysis was done using Stat View 5.0 (Cary, NC) and SPSS v 16.0 (Chicago, IL).

Results

IL13Rα2 is overexpressed in ACC

The expression of IL13Rα2 mRNA was significantly higher in ACC as compared to normal adrenocortical tissue and benign adrenocortical tumors ($p<0.001$) (Figure 1A). In addition, IL13Rα2 mRNA expression level was also higher in metastatic and recurrent tumors as compared to normal adrenocortical tissue but was lower than primary ACC ($p<0.001$). Consistent with the mRNA expression data (Figure 1A), IL13Rα2 protein expression was also higher in ACC and benign adrenocortical tumor samples as compared to normal adrenocortical tissue (Figure 1B). Semiquantitative scoring found a significant difference between normal vs. benign or malignant tumors ($p<0.05$) (Figure 1C). IL13Rα2 was specifically and uniformly overexpressed in malignant cells but not in adjacent normal tissues.

IL-13 signals through IL13Rα2 and influences ACC cell invasion

Given the high expression of IL13Rα2 in ACC we next determined whether the receptor was biologically active. Specifically, since IL-13 is thought to signal through IL13Rα2, we attempted to evaluate the responsiveness of the IL13Rα2 overexpressing ACC cell line, NCI-H295R, to IL-13 ligand. We found significant induction of IL13Rα2 in cells treated with 50 ng/ml of IL-13 ligand (Figure 2A). In addition, IL13Rα2 immunofluorescence, indicated that the receptor was expressed predominantly in cell membrane and cytoplasm (Figure 2A).

To better understand the potential biological effects of IL-13 and *IL13Rα2* signaling in ACC cells, we also evaluated invasion as a measure of metastatic potential in NCI-H295R cells in the presence or absence of IL-13. It has been previously shown in pancreatic cancer cell lines that IL-13 signals through *IL13Rα2* to promote invasion [28]. To assess this

response in ACC, we used siRNA to knockdown *IL13Rα2* expression in NCI-H295R cells. This approach resulted in 84–88% reduction in mRNA expression within 24 hours as compared to negative control group, which lasted up to 7 days (Figure 2B). Furthermore, we observed a 75% decrease in cell surface protein expression of IL13Rα2 as compared to negative control after 7 days of transfection (Figure 3A). NCI-H295R cells were incubated with IL-13 to assess invasion. We found the number of invading cells increased by 15% with IL-13 treatment (Figure 3B). In addition, after quantitation, the number of invaded cells decreased by 44.7% in *IL13Rα2* silenced group as compared to siRNA negative control in the presence of IL-13 (p=0.007) and decreased by 30% in the absence of IL-13 (p=0.006) (Figure 3C). These results suggest that IL-13 signals through *IL13Rα2* and promotes ACC cell invasion. In addition, there was a 28.5–33% decrease in cell proliferation after days 11 and 14 of *IL13Rα2* knockdown as compared to negative control (p<0.001) (Figure 3D).

IL13Rα2 positive ACC cell lines are sensitive to IL-13-PE cytotoxin

Given that IL13Rα2 is overexpressed in ACC, we evaluated its potential as a therapeutic target for ACC *in vitro* and *in vivo*. The sensitivity of two ACC cell lines (NCI-H295R with high *IL13Rα2* expression and SW13 with low *IL13Rα2* expression) to a highly specific immunotoxin IL-13-PE was determined (Figure 4A). In addition, a renal cell carcinoma cell line, PM-RCC with high *IL13Rα2* mRNA expression was used as positive control. The IC_{50} for IL-13-PE was significantly lower (1.3 ng/ml and 0.2 ng/ml) in NCI-H295R and PM-RCC cells with high IL13Rα2 expression (Figure 4B) than the IC_{50} of 600 ng/ml in SW13 cells, which have, lower IL13Rα2 expression (p<0.05) (Figure 4C). The IL-13-PE at IC_{50} was also administered in negative control and siRNA transfected cells to evaluate the specificity of IL-13-PE to IL13Rα2. The treatment resulted in loss of sensitivity in siRNA transfected cells as compared to negative controls (Figure 4D). The IC_{50} was determined using protein synthesis inhibition assay and was significantly lower in negative control and untreated (0.9 ng/ml, 2 ng/ml) as compared to siRNA treated group (≥1000 ng/ml) (p<0.05) (Figure 4E).

To further confirm the cytotoxic effect of IL-13-PE in a three-dimensional model that better mimics solid tumors, it was also administered to NCI-H295R tumor spheroids. NCI-H295R cells were cultured for one week to form spheroids, after which the spheroids were treated with different concentrations of IL-13-PE for two weeks. We observed a significant reduction in the spheroid size and disaggregation of cells during treatment within one week of treatment (Figure 4F).

Treatment with IL-13-PE causes tumor regression and prolonged survival in xenograft model of ACC

Based on the profound effect of IL-13-PE on ACC cell line growth *in vitro*, the efficacy of IL-13-PE in ACC xenografts was determined in athymic nude mice NCr-nu/nu model. Mice were injected with NCI-H295R cells and treatment was initiated after the tumors reached a size of ~50–60 mm^3. After 14 days, mice were randomized into five groups. The routes of IL-13-PE administration were all well tolerated with no observed toxicity by histological examination of vital organs (liver, kidney, spleen and lung). In addition, there was no significant weight difference among the groups. Nineteen days after treatment, mice with one and two week of IT treatment (group I and II) showed a 70% reduction in tumor size as compared to vehicle control group (group1V) (p<0.05) (Figure 5A), while the IP group (group III) showed a 47% reduction by day 25 as compared to vehicle control (group V) (p<0.05) (Figure 5B). We also found significantly longer survival in group I, II and III (108, 106 and 111 days, respectively) as compared to group IV and V [(69 and 84 days) (p<0.05). In addition, histological analysis in the IP and IT control group demonstrated presence of viable cells (Figure 5C) while tumors treated with IL-13-PE showed evidence of necrosis

(Figure 5C). We found no significant difference in IL13Rα mRNA and protein expression between IL-13-PE treated and vehicle control tumor samples from the mice.

Discussion

We analyzed, for the first time, *IL13Rα2* expression and it's biologic significance as a therapeutic target in ACC. Our results demonstrate that *IL13Rα2* is overexpressed in ACC and is an excellent therapeutic target. *IL13Rα2* knockdown in ACC cells resulted in suppression of invasion, suggesting that it may influence cell invasive phenotype in ACC. Our data also demonstrates that *IL13Rα2* is a novel therapeutic target for the treatment of ACC with IL-13-PE.

Our study demonstrates IL13Rα2 mRNA and protein overexpression in ACC as has been observed in other malignancies [12; 14; 16; 27; 29; 30]. Interestingly, *IL13Rα2* mRNA expression was lower in tumors from a cohort of metastatic and recurrent ACC patients who received prior systemic chemotherapy before surgical resection but still well over 5-fold higher than in normal adrenocortical tissue. These results suggest that *IL13Rα2* expression may vary because of treatment. Thus, given that IL13Rα2 expression is low or absent in normal organs it would be reasonable to consider IL-13-PE therapy in patients with metastatic or locally advanced ACC.

Given the overexpression of *IL13Rα2* in ACC, we were interested in evaluating if the receptor was functional in ACC. Using siRNA knockdown, the number of invading cells was reduced significantly as compared to negative control. In addition, incubation of cells with IL-13 ligand increased the invasion as compared to negative control group and the loss of effect in *IL13Rα2* silenced cells. Therefore, these results suggest that *IL13Rα2* is involved in ACC invasion and *IL13Rα2* mediates IL-13 signaling in NCI-H295R cells. In addition, invasive feature (capsular invasion) was observed in histology of malignant tumors with higher *IL13Rα2* overexpression. Previously, it has been shown that IL-13 activates AP-1 transcription factor that in turn activates matrix metalloproteinases (MMPs) and thereby may influence metastatic potential in pancreatic cancer cells [28]. MMPs are associated with tumor invasion and metastasis of malignant tumors with different histogenetic origin [31; 32]. The present findings are also supported by other studies that found IL13Rα2 is elevated in breast cancer metastasis and glioma cells with mutant epidermal growth factor receptor [28; 33; 34]. Our findings indicate that IL-13 mediates signaling through IL13Rα2, and influences cellular invasion and proliferation in ACC cells.

Given the specific overexpression of IL13Rα2 in ACC and the lack of IL13Rα2 expression in the vast majority of normal tissues, we were interested in evaluating its role as a therapeutic target. IL-13-PE has been shown to inhibit the growth of different cancer cells *in vitro* and *in vivo* [26; 27]. We tested the sensitivity and specificity of ACC cell lines to IL-13-PE in monolayer culture and found that IC_{50} was low for NCI-H295R cell line positive for *IL13Rα2* as compared to SW13, a receptor negative cell line. In addition, IL-13-PE treatment led to significant decrease in the sensitivity and IC_{50} in siRNA group of transfected cells (≥1000 ng/ml) than in negative control group (0.9 ng/ml). These results suggest that the IL-13-PE is highly specific to IL13Rα2. With these encouraging results, we also evaluated sensitivity in three-dimensional *in vitro* culture of spheroids to confirm the efficacy of IL-13-PE in ACC. The spheroid model resembles a solid tumor and is used for studying therapeutic drug testing, understanding tumor growth, and cellular differentiation and invasion [35; 36]. Our results showed a dramatic effect on tumor spheroids at very low concentrations of IL-13-PE, which confirms the efficacy and specificity of IL-13-PE to IL13Rα2 positive ACC cells.

Based on the positive results of cytoxicity in monolayer and spheroid culture, IL-13-PE efficacy was also determined in an *in vivo* model of subcutaneous xenografts. ACC xenografts were developed using NCI-H295R cells and administration of IL-13-PE through IT and IP routes of injection resulted in significant reduction (70% and 47%, respectively) in established tumors within three weeks with no observable signs of toxicity. IT injection was more effective likely due the direct route of administration as longer treatment (higher cumulative dose) with this route of administration resulted in no significant difference tumor reduction. This result is in concordance with the previous studies in other IL13Rα2 positive tumor types such as, glioma, renal cell carcinoma and pancreatic adenocarcinoma [15; 17; 27; 37]. In addition, histological analysis of the xenograft tumors revealed significant necrosis in tumors treated with IL-13-PE while vehicle treated tumors showed evidence of viable cells. Thus, as seen in previous studies using IL-13-PE based immunotoxin, our results indicate that this agent seems to cause cell death and tumor necrosis [38; 39; 40].

In summary, this is the first study demonstrating that IL13Rα2 is overexpressed in ACC and is a novel therapeutic target for ACC. IL-13-PE immunotoxin is specific to *IL13Rα2* and significantly inhibits tumor growth *in vitro* and in a human xenograft ACC animal model. Therefore, our results suggest that *IL13Rα2* may be used as novel target and supports that IL-13-PE immunotoxin may be tested in a clinical trial in patients who have advanced and metastatic ACC.

REFERENCES

1. Bilimoria KY, Shen WT, Elaraj D, Bentrem DJ, Winchester DJ, Kebebew E, Sturgeon C. Adrenocortical carcinoma in the United States: treatment utilization and prognostic factors. Cancer. 2008; 113:3130–3136. [PubMed: 18973179]
2. Icard P, Louvel A, Le Charpentier M, Chapuis Y. Adrenocortical tumors with oncocytic cells: benign or malignant? Ann Chir. 2001; 126:249–253. [PubMed: 11340712]
3. Favia G, Lumachi F, Carraro P, D'Amico DF. Adrenocortical carcinoma. Our experience. Minerva Endocrinol. 1995; 20:95–99. [PubMed: 7651289]
4. Wajchenberg BL, Albergaria Pereira MA, Medonca BB, Latronico AC, Campos Carneiro P, Alves VA, Zerbini MC, Liberman B, Carlos Gomes G, Kirschner MA. Adrenocortical carcinoma: clinical and laboratory observations. Cancer. 2000; 88:711–736. [PubMed: 10679640]
5. Kebebew E, Reiff E, Duh QY, Clark OH, McMillan A. Extent of disease at presentation and outcome for adrenocortical carcinoma: have we made progress? World J Surg. 2006; 30:872–878. [PubMed: 16680602]
6. Lombardi CP, Raffaelli M, Pani G, Maffione A, Princi P, Traini E, Galeotti T, Rossi ED, Fadda G, Bellantone R. Gene expression profiling of adrenal cortical tumors by cDNA macroarray analysis. Results of a preliminary study. Biomed Pharmacother. 2006; 60:186–190. [PubMed: 16677799]
7. Slater EP, Diehl SM, Langer P, Samans B, Ramaswamy A, Zielke A, Bartsch DK. Analysis by cDNA microarrays of gene expression patterns of human adrenocortical tumors. Eur J Endocrinol. 2006; 154:587–598. [PubMed: 16556722]
8. Velazquez-Fernandez D, Laurell C, Geli J, Hoog A, Odeberg J, Kjellman M, Lundeberg J, Hamberger B, Nilsson P, Backdahl M. Expression profiling of adrenocortical neoplasms suggests a molecular signature of malignancy. Surgery. 2005; 138:1087–1094. [PubMed: 16360395]
9. Giordano TJ, Thomas DG, Kuick R, Lizyness M, Misek DE, Smith AL, Sanders D, Aljundi RT, Gauger PG, Thompson NW, Taylor JM, Hanash SM. Distinct transcriptional profiles of adrenocortical tumors uncovered by DNA microarray analysis. Am J Pathol. 2003; 162:521–531. [PubMed: 12547710]
10. Fernandez-Ranvier GG, Weng J, Yeh RF, Khanafshar E, Suh I, Barker C, Duh QY, Clark OH, Kebebew E. Identification of biomarkers of adrenocortical carcinoma using genomewide gene expression profiling. Arch Surg. 2008; 143:841–846. discussion 846. [PubMed: 18794420]
11. Suh I, Guerrero MA, Kebebew E. Gene-expression profiling of adrenocortical carcinoma. Expert Rev Mol Diagn. 2009; 9:343–351. [PubMed: 19441174]

12. Husain SR, Obiri NI, Gill P, Zheng T, Pastan I, Debinski W, Puri RK. Receptor for interleukin 13 on AIDS-associated Kaposi's sarcoma cells serves as a new target for a potent Pseudomonas exotoxin-based chimeric toxin protein. Clin Cancer Res. 1997; 3:151–156. [PubMed: 9815666]
13. Joshi BH, Leland P, Puri RK. Identification and characterization of interleukin-13 receptor in human medulloblastoma and targeting these receptors with interleukin-13-pseudomonas exotoxin fusion protein. Croat Med J. 2003; 44:455–462. [PubMed: 12950150]
14. Kawakami M, Kawakami K, Kasperbauer JL, Hinkley LL, Tsukuda M, Strome SE, Puri RK. Interleukin-13 receptor alpha2 chain in human head and neck cancer serves as a unique diagnostic marker. Clin Cancer Res. 2003; 9:6381–6388. [PubMed: 14695138]
15. Puri RK, Leland P, Obiri NI, Husain SR, Kreitman RJ, Haas GP, Pastan I, Debinski W. Targeting of interleukin-13 receptor on human renal cell carcinoma cells by a recombinant chimeric protein composed of interleukin-13 and a truncated form of Pseudomonas exotoxin A (PE38QQR). Blood. 1996; 87:4333–4339. [PubMed: 8639793]
16. Kioi M, Kawakami M, Shimamura T, Husain SR, Puri RK. Interleukin-13 receptor alpha2 chain: a potential biomarker and molecular target for ovarian cancer therapy. Cancer. 2006; 107:1407–1418. [PubMed: 16902988]
17. Shimamura T, Fujisawa T, Husain SR, Joshi B, Puri RK. Interleukin 13 mediates signal transduction through interleukin 13 receptor alpha2 in pancreatic ductal adenocarcinoma: role of IL-13 Pseudomonas exotoxin in pancreatic cancer therapy. Clin Cancer Res. 16:577–586. [PubMed: 20068108]
18. Kioi M, Shimamura T, Nakashima H, Hirota M, Tohnai I, Husain SR, Puri RK. IL-13 cytotoxin has potent antitumor activity and synergizes with paclitaxel in a mouse model of oral squamous cell carcinoma. Int J Cancer. 2009; 124:1440–1448. [PubMed: 19065664]
19. Kawakami K, Taguchi J, Murata T, Puri RK. The interleukin-13 receptor alpha2 chain: an essential component for binding and internalization but not for interleukin-13-induced signal transduction through the STAT6 pathway. Blood. 2001; 97:2673–2679. [PubMed: 11313257]
20. Rahaman SO, Sharma P, Harbor PC, Aman MJ, Vogelbaum MA, Haque SJ. IL-13R(alpha)2, a decoy receptor for IL-13 acts as an inhibitor of IL-4-dependent signal transduction in glioblastoma cells. Cancer Res. 2002; 62:1103–1109. [PubMed: 11861389]
21. O'Shea JJ, Gadina M, Schreiber RD. Cytokine signaling in 2002: new surprises in the Jak/Stat pathway. Cell. 2002; 109(Suppl):S121–S131. [PubMed: 11983158]
22. Fichtner-Feigl S, Strober W, Kawakami K, Puri RK, Kitani A. IL-13 signaling through the IL-13alpha2 receptor is involved in induction of TGF-beta1 production and fibrosis. Nat Med. 2006; 12:99–106. [PubMed: 16327802]
23. Wynn TA. IL-13 effector functions. Annu Rev Immunol. 2003; 21:425–456. [PubMed: 12615888]
24. Pastan I, Hassan R, FitzGerald DJ, Kreitman RJ. Immunotoxin treatment of cancer. Annu Rev Med. 2007; 58:221–237. [PubMed: 17059365]
25. Joshi BH, Puri RK. Optimization of expression and purification of two biologically active chimeric fusion proteins that consist of human interleukin-13 and Pseudomonas exotoxin in Escherichia coli. Protein Expr Purif. 2005; 39:189–198. [PubMed: 15642470]
26. Joshi BH, Kawakami K, Leland P, Puri RK. Heterogeneity in interleukin-13 receptor expression and subunit structure in squamous cell carcinoma of head and neck: differential sensitivity to chimeric fusion proteins comprised of interleukin-13 and a mutated form of Pseudomonas exotoxin. Clin Cancer Res. 2002; 8:1948–1956. [PubMed: 12060640]
27. Kioi M, Seetharam S, Puri RK. Targeting IL-13Ralpha2-positive cancer with a novel recombinant immunotoxin composed of a single-chain antibody and mutated Pseudomonas exotoxin. Mol Cancer Ther. 2008; 7:1579–1587. [PubMed: 18566228]
28. Fujisawa T, Joshi B, Nakajima A, Puri RK. A novel role of interleukin-13 receptor alpha2 in pancreatic cancer invasion and metastasis. Cancer Res. 2009; 69:8678–8685. [PubMed: 19887609]
29. Joshi BH, Plautz GE, Puri RK. Interleukin-13 receptor alpha chain: a novel tumor-associated transmembrane protein in primary explants of human malignant gliomas. Cancer Res. 2000; 60:1168–1172. [PubMed: 10728667]
30. Debinski W, Gibo DM. Molecular expression analysis of restrictive receptor for interleukin 13, a brain tumor-associated cancer/testis antigen. Mol Med. 2000; 6:440–449. [PubMed: 10952023]

31. Basset P, Okada A, Chenard MP, Kannan R, Stoll I, Anglard P, Bellocq JP, Rio MC. Matrix metalloproteinases as stromal effectors of human carcinoma progression: therapeutic implications. Matrix Biol. 1997; 15:535–541. [PubMed: 9138286]
32. Johnsen M, Lund LR, Romer J, Almholt K, Dano K. Cancer invasion and tissue remodeling: common themes in proteolytic matrix degradation. Curr Opin Cell Biol. 1998; 10:667–671. [PubMed: 9818179]
33. Minn AJ, Gupta GP, Siegel PM, Bos PD, Shu W, Giri DD, Viale A, Olshen AB, Gerald WL, Massague J. Genes that mediate breast cancer metastasis to lung. Nature. 2005; 436:518–524. [PubMed: 16049480]
34. Lal A, Glazer CA, Martinson HM, Friedman HS, Archer GE, Sampson JH, Riggins GJ. Mutant epidermal growth factor receptor up-regulates molecular effectors of tumor invasion. Cancer Res. 2002; 62:3335–3339. [PubMed: 12067969]
35. Sutherland RM, McCredie JA, Inch WR. Growth of multicell spheroids in tissue culture as a model of nodular carcinomas. J Natl Cancer Inst. 1971; 46:113–120. [PubMed: 5101993]
36. Mueller-Klieser W. Tumor biology and experimental therapeutics. Crit Rev Oncol Hematol. 2000; 36:123–139. [PubMed: 11033302]
37. Vogelbaum MA, Sampson JH, Kunwar S, Chang SM, Shaffrey M, Asher AL, Lang FF, Croteau D, Parker K, Grahn AY, Sherman JW, Husain SR, Puri RK. Convection-enhanced delivery of cintredekin besudotox (interleukin-13-PE38QQR) followed by radiation therapy with and without temozolomide in newly diagnosed malignant gliomas: phase 1 study of final safety results. Neurosurgery. 2007; 61:1031–1037. discussion 1037–1038. [PubMed: 18091279]
38. Keppler-Hafkemeyer A, Brinkmann U, Pastan I. Role of caspases in immunotoxin-induced apoptosis of cancer cells. Biochemistry. 1998; 37:16934–16942. [PubMed: 9836586]
39. Hafkemeyer P, Brinkmann U, Gottesman MM, Pastan I. Apoptosis induced by Pseudomonas exotoxin: a sensitive and rapid marker for gene delivery in vivo. Hum Gene Ther. 1999; 10:923–934. [PubMed: 10223726]
40. Kawakami M, Kawakami K, Puri RK. Apoptotic pathways of cell death induced by an interleukin-13 receptor-targeted recombinant cytotoxin in head and neck cancer cells. Cancer Immunol Immunother. 2002; 50:691–700. [PubMed: 11862421]

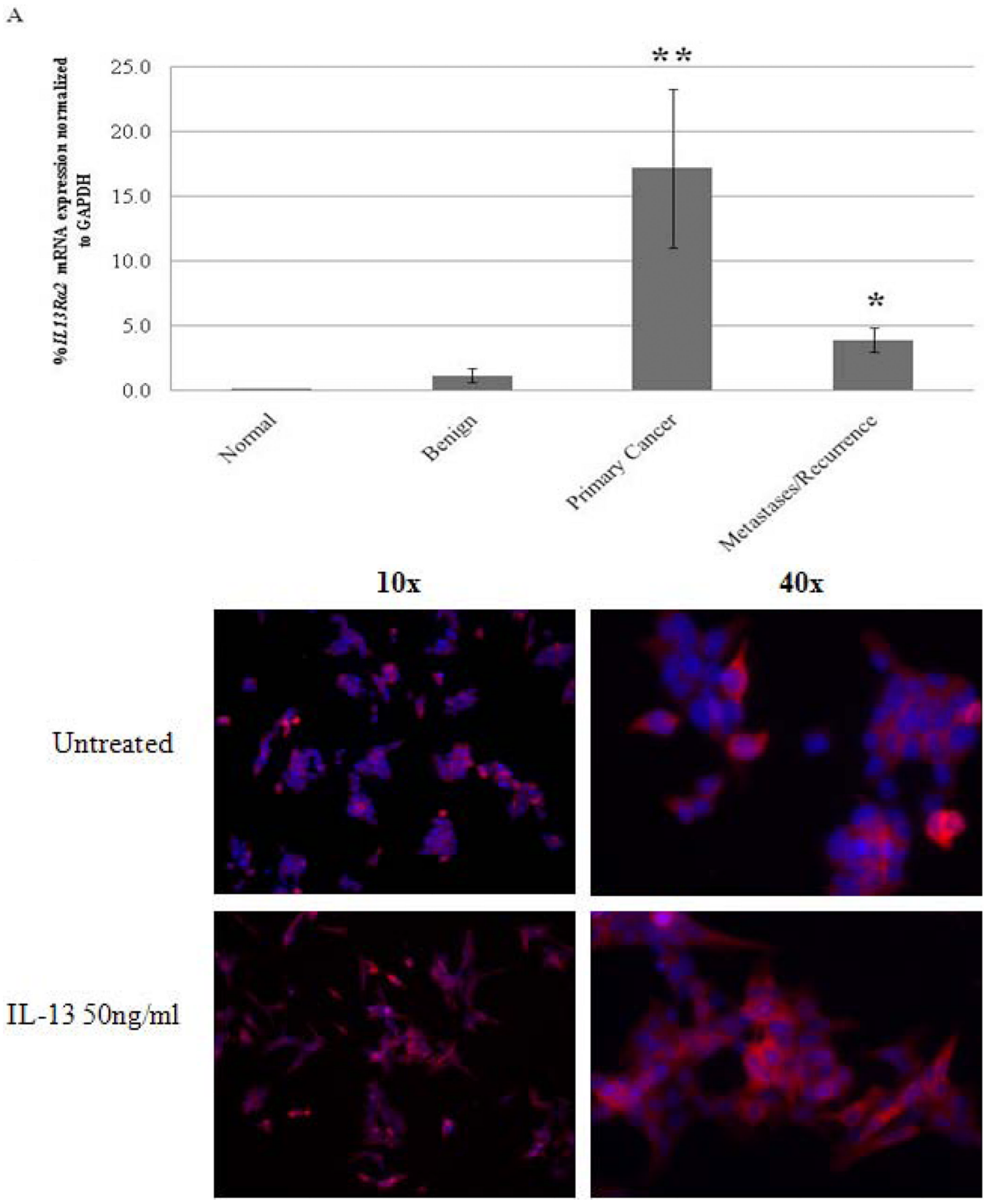

Figure 1.

IL13Rα2 mRNA expression in ACC. **A**) *IL13Rα2* mRNA expression in normal adrenal cortex (n = 21), benign adrenocortical tumors (n = 78), primary ACC (n = 10), and metastatic and recurrent ACC (n=25). Statistical significant difference was indicated by an asterisk (*) ($p<0.05$, One-Way ANOVA post-hoc tests). **Primary ACC or benign vs. normal ($p < 0.001$) and *primary ACC vs. metastases ($p < 0.001$). **B**) Immunohistochemistry for IL13Rα2 protein expression in normal adrenocortical tissue (1–2), benign tumors (3–4) and malignant ACC (5–6). (7–8) The corresponding H&E image of the malignant sample representing invasive features. Representative images are shown for each category at 10X and 20X magnifications. Arrows indicate the positive cytoplasmic and membrane staining for *IL13Rα2*. **C**) Semiquantitative IL13Rα2 IHC scores are shown in the normal (n=7), benign (n=8) and ACC (n=6) samples. Columns represent the average score (obtained from two individual investigators) ± standard deviation. Black asterisk indicates significant difference between benign and normal while red asterisk indicate the difference between malignant and normal tissue samples.

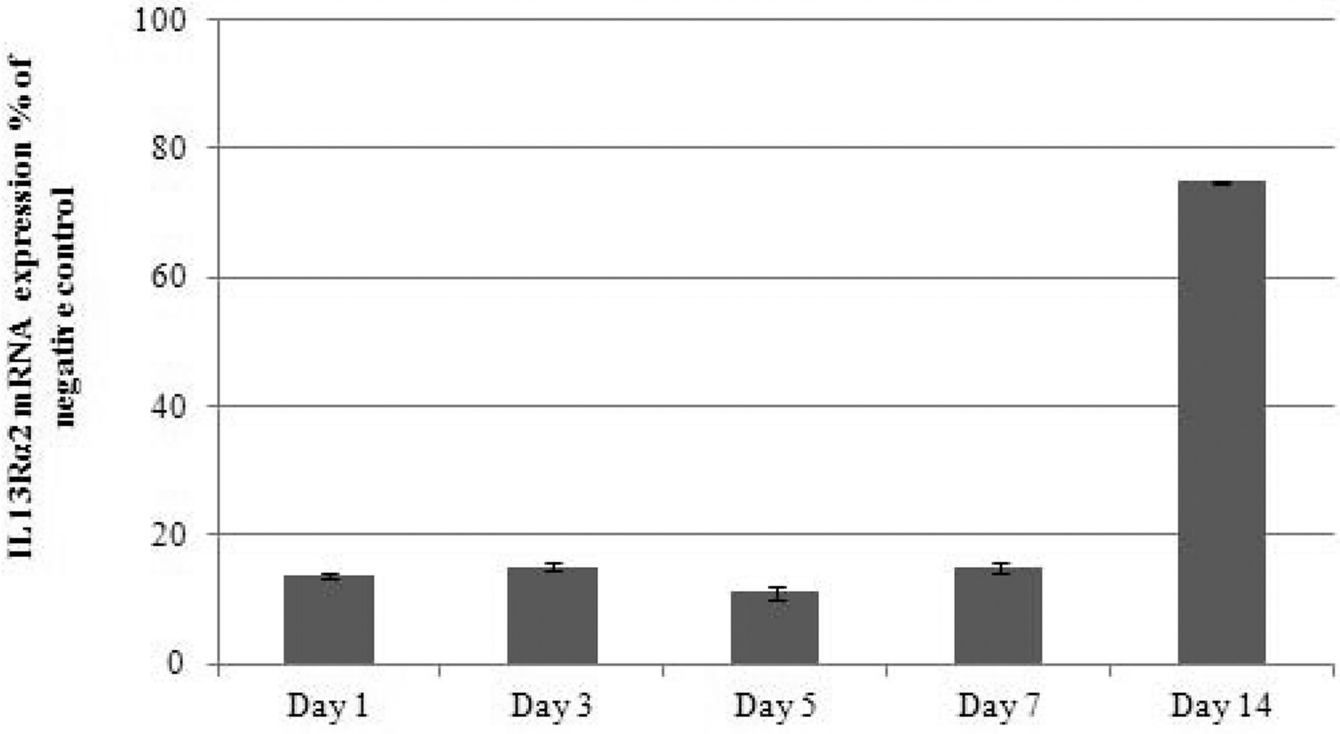

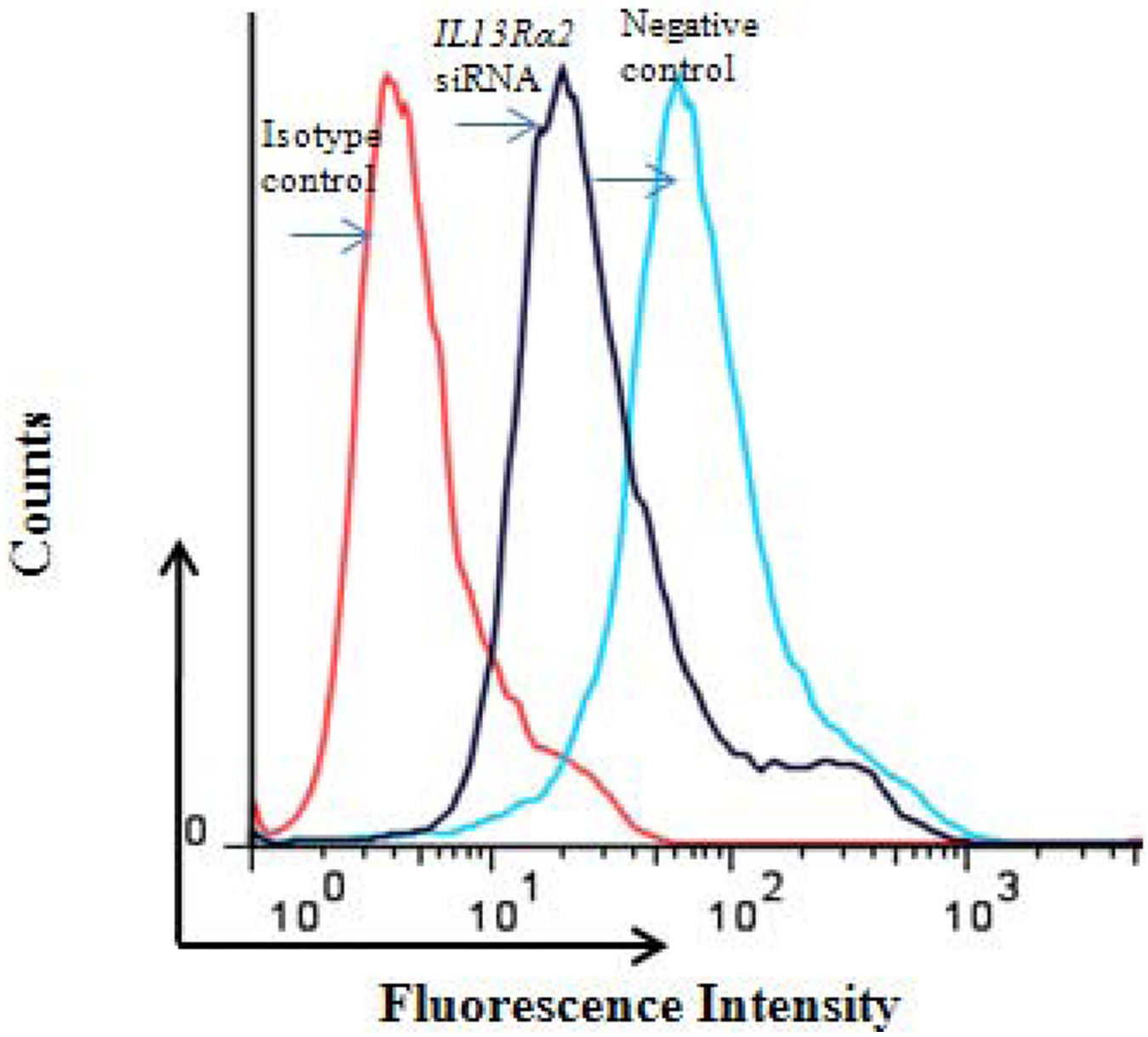

Figure 2.

IL-13 increases *IL13Rα2* expression in H295R cells. **A**) Exposure of IL-13 at 50 ng/ml increased *IL13Rα2* expression after 48 hours as analyzed by immunoflouroscence. Nuclei were stained by DAPI (blue), red color indicates *IL13Rα2* expression. The upper panel image represents untreated cells and the lower panel represents treated cells at 10X and 40X magnification. **B)** *IL13Rα2* siRNA knockdown in the NCI-H295R adrenocortical carcinoma cell line. Transient transfection was done in H295R cells using *IL13Rα2* siRNA and negative control and cells were analyzed for mRNA expression after day 1, 3, 5 and 7 of treatment. Columns represent remaining *IL13Rα2* mRNA expression percentage relative to negative control ± standard deviation of four experiments.

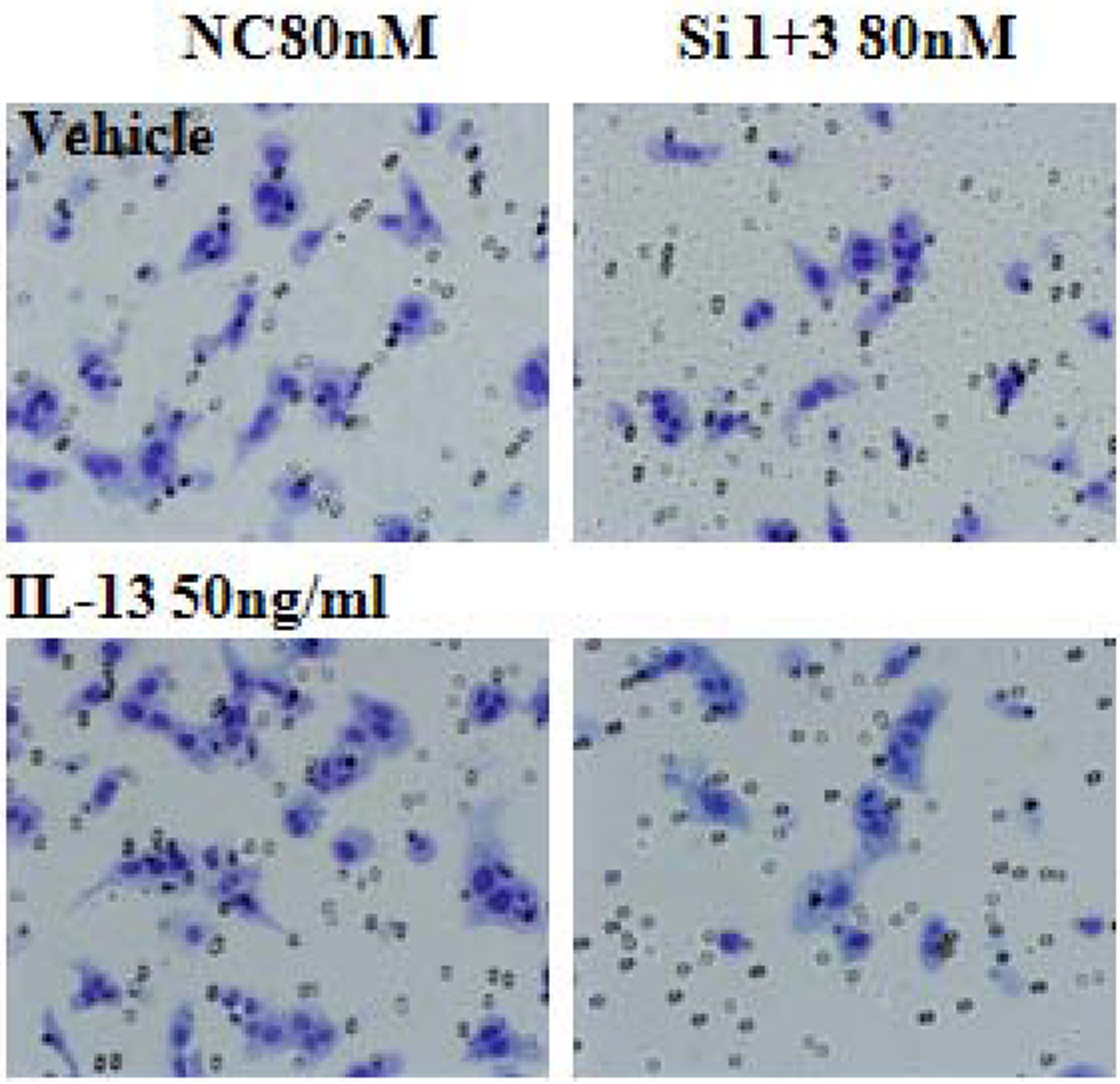

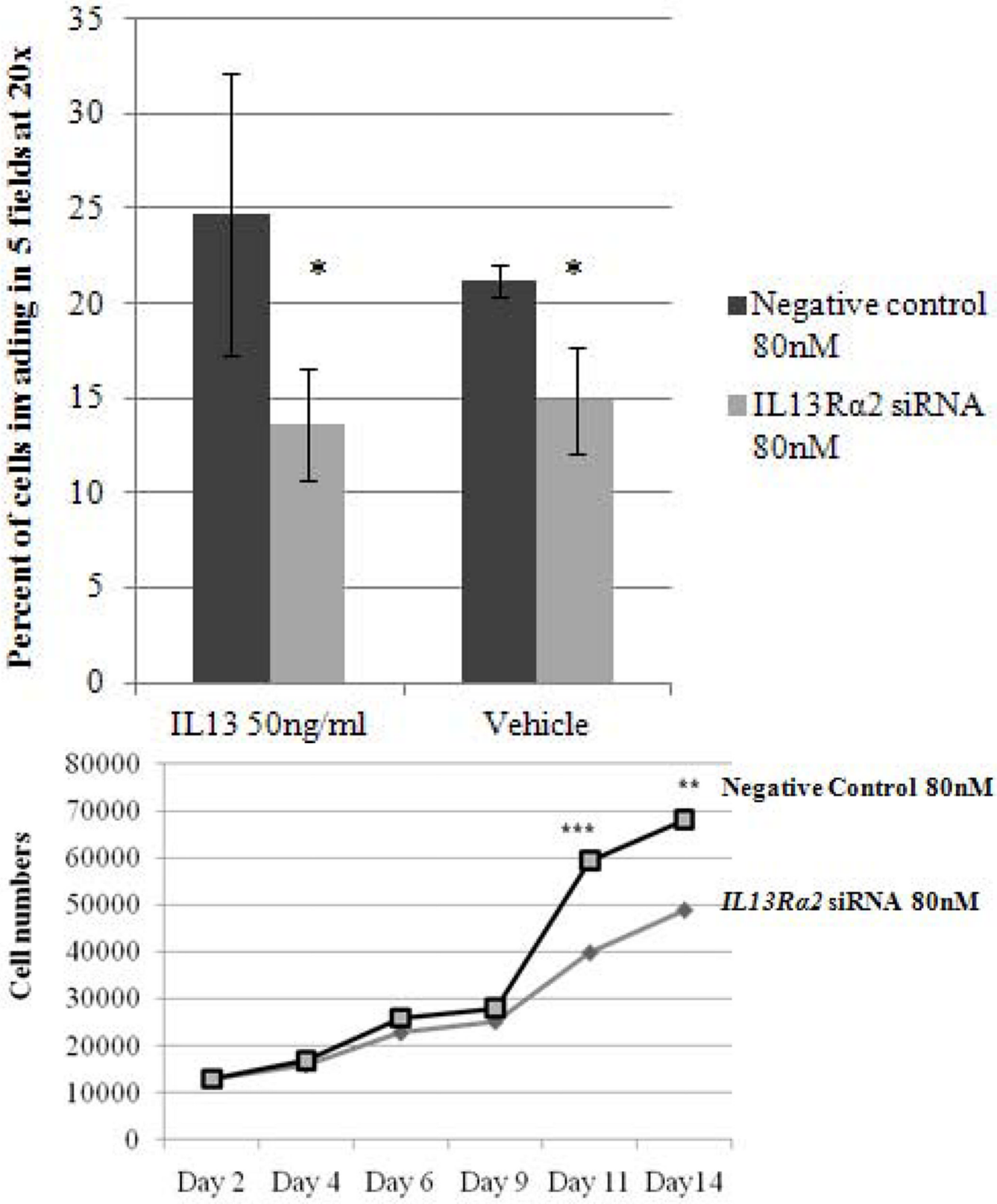

Figure 3.

A) *IL13Rα2* protein expression at the cell surface in siRNA transfected cells was assessed by flow cytometry. Representative histograms demonstrating cell surface expression of *IL13Rα2* after 7 days of *IL13Rα2* siRNA or negative control treatment. The x-axis indicates FITC fluorescence intensity and Y-axis indicates cell count. The red color represents the isotype control, and the black and blue lines represent *IL13Rα2* siRNA knockdown and negative control cells, respectively. **B**) *IL13Rα2* siRNA knockdown reduced invasion in NCI-H295R cell line. Representative images are shown at 20X. **C)** Quantitative analysis of the number of cells invading with and without *IL13Rα2* siRNA as compared to siRNA negative control group. Columns represent the mean ± standard deviation (SD) of three independent experiments performed in triplicate. *$p<0.05$ *IL13Rα2* siRNA vs. siRNA negative control. **D**) *IL13Rα2* siRNA knockdown and cell proliferation in the NCI-H295R cell line. The distribution of number of cells for the *IL13Rα2* siRNA treated and negative control treated groups are shown at indicated time points (significant values are indicated by asterisk (*) (*** $p<0.001$; ** $p<0.01$; relative to negative control). Error bars represent ± standard error of mean and is representative of four experiments.

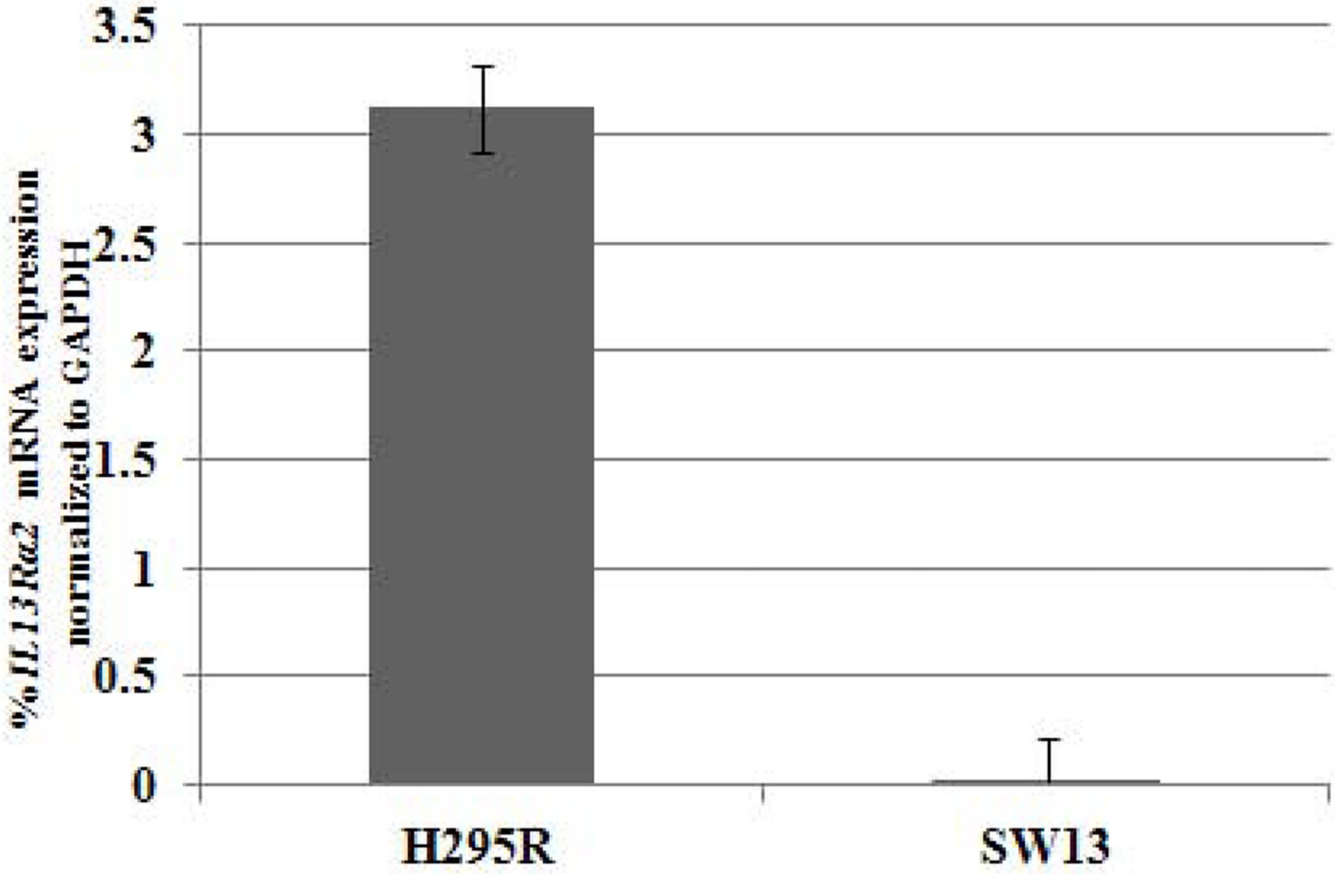

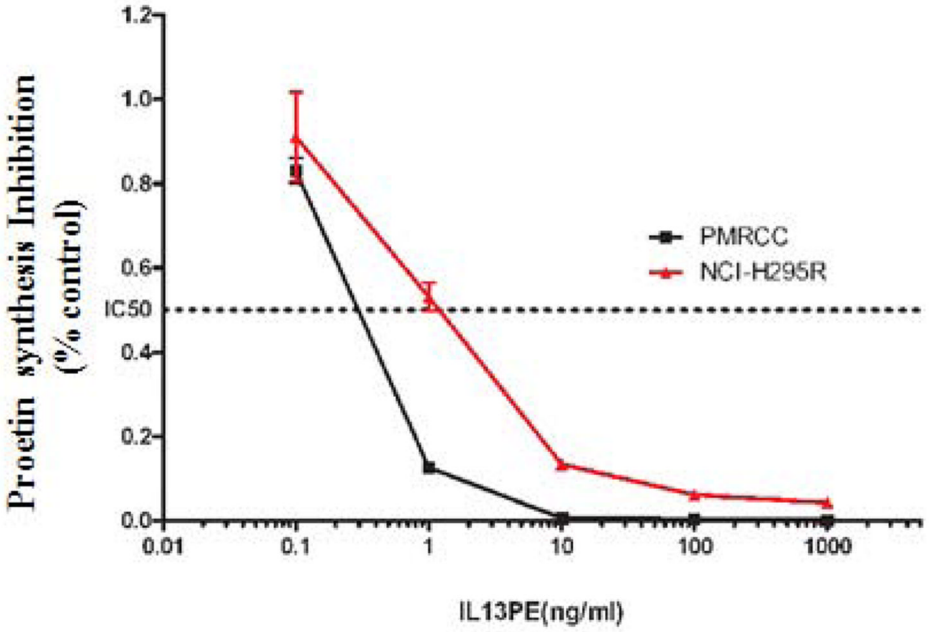

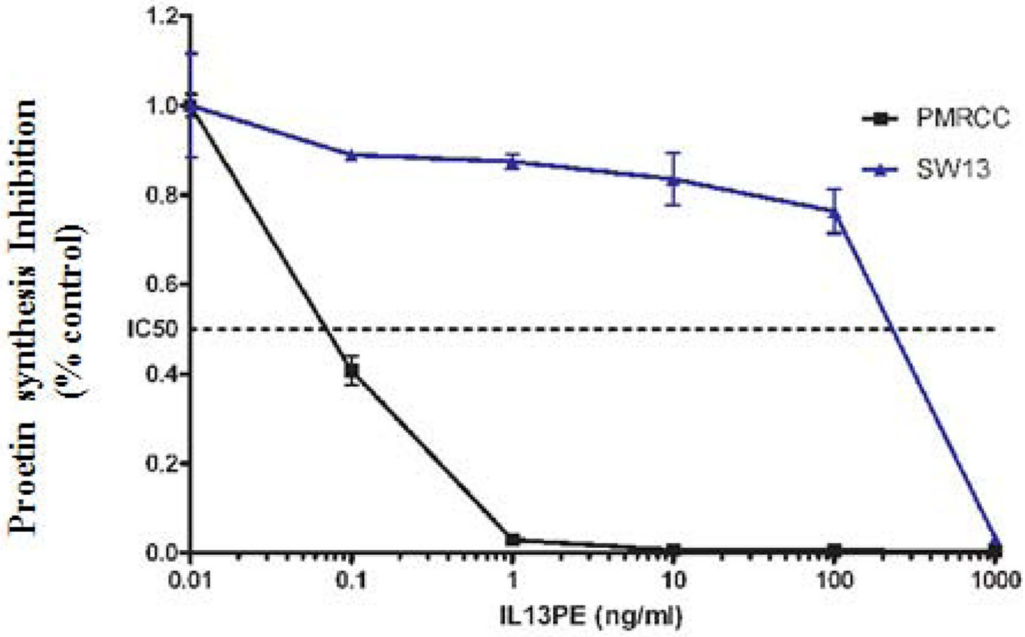

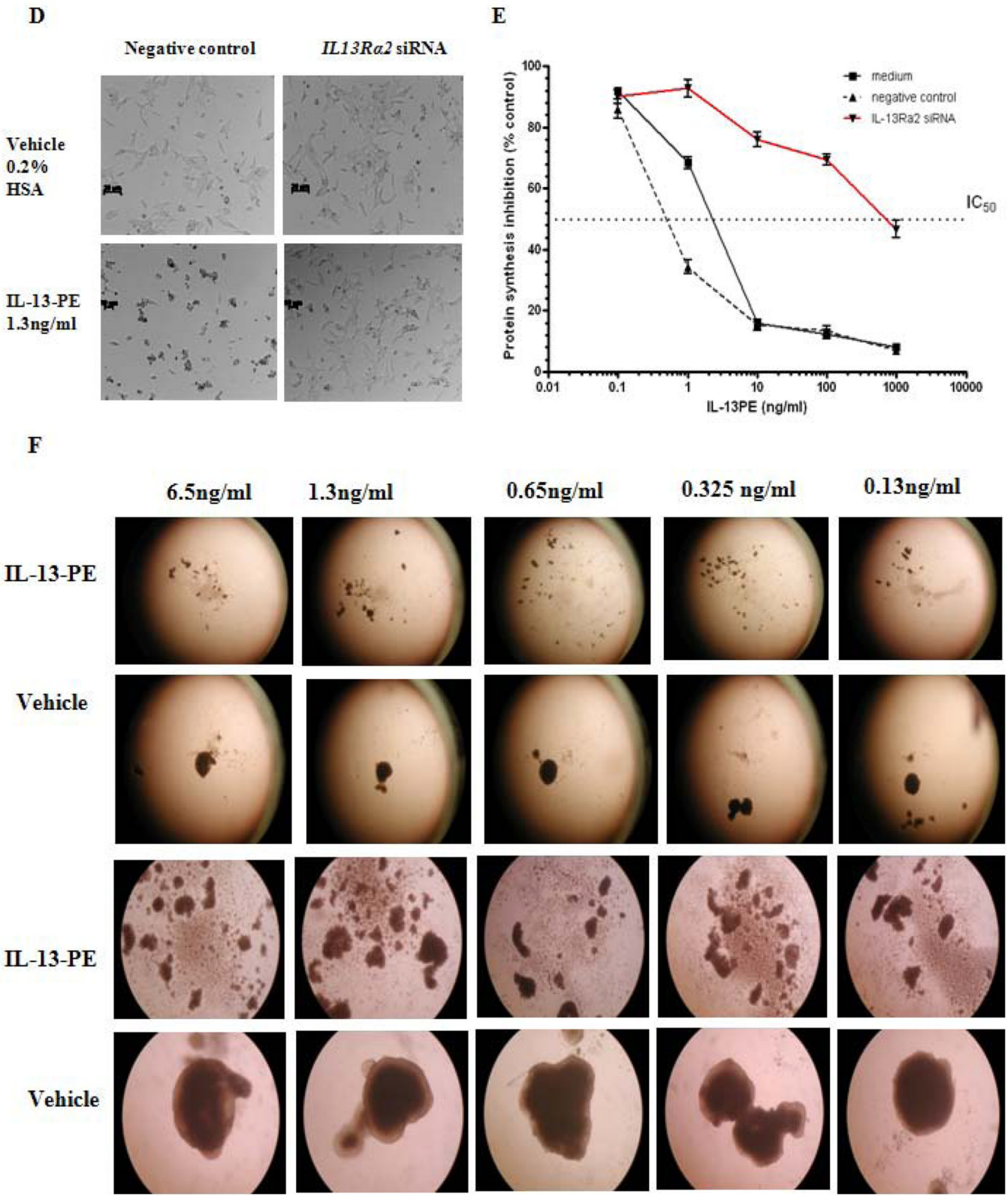

Figure 4.

IL13Rα2 positive H295R cells are sensitive to IL-13-PE. **A**) *IL13Rα2* mRNA expression in ACC cell lines (H295R and SW13). Y axis represents % *IL13Rα2* mRNA expression relative to GAPDH. Protein synthesis inhibition assay was done to assess the cytotoxicity of IL-13-PE to H295R (**B**) and SW13 (**C**) cells. PM-RCC cells (renal carcinoma cell line) were used as positive control. Mean ± SD of quadruplicate determination. **D**) IL-13-PE was administered at concentration of 1.3 ng/ml to cells with *IL13Rα2* knockdown and negative control. Upper panel represents negative control and siRNA knockdown cells treated with vehicle (0.2% HSA) and lower panel represents the cells treated with IL-13-PE. All images are at 10X magnification and representative of two experiments done in duplicates. **E**) Protein synthesis inhibition assay was done to assess the cytotoxicity of IL-13-PE to H295R transfected cells with *IL13Rα2 siRNA* and negative control used at 80 nM concentration. **F)** Effect of IL-13-PE in H295R spheroids. Spheroids were treated with IL-13-PE and vehicle at different concentrations of 0.13 ng/ml to 6.5 ng/ml. Upper panel represents IL-13PE treatment at 12.5X magnification and lower panel represents vehicle treatment at 50X magnification.

A

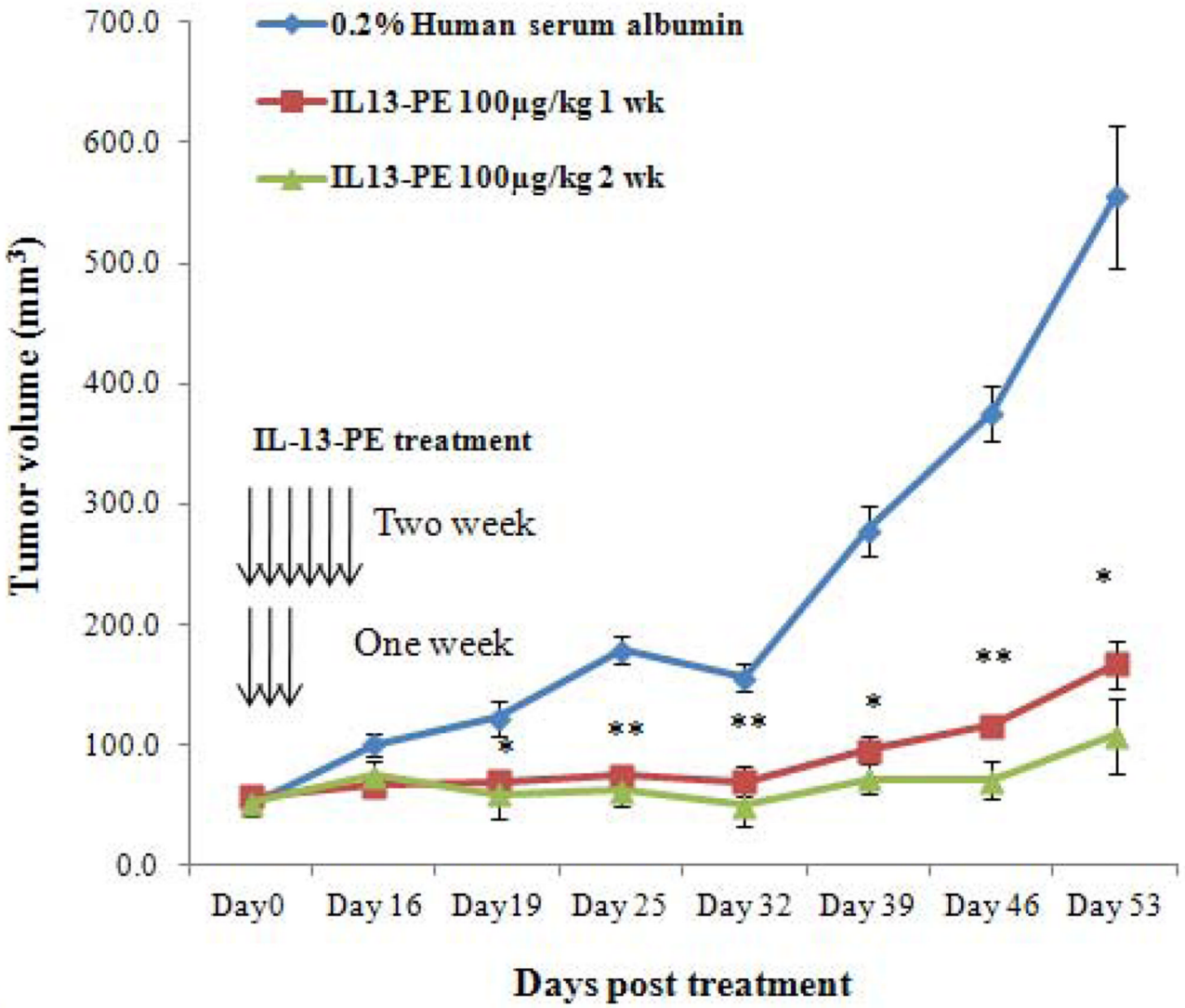

B

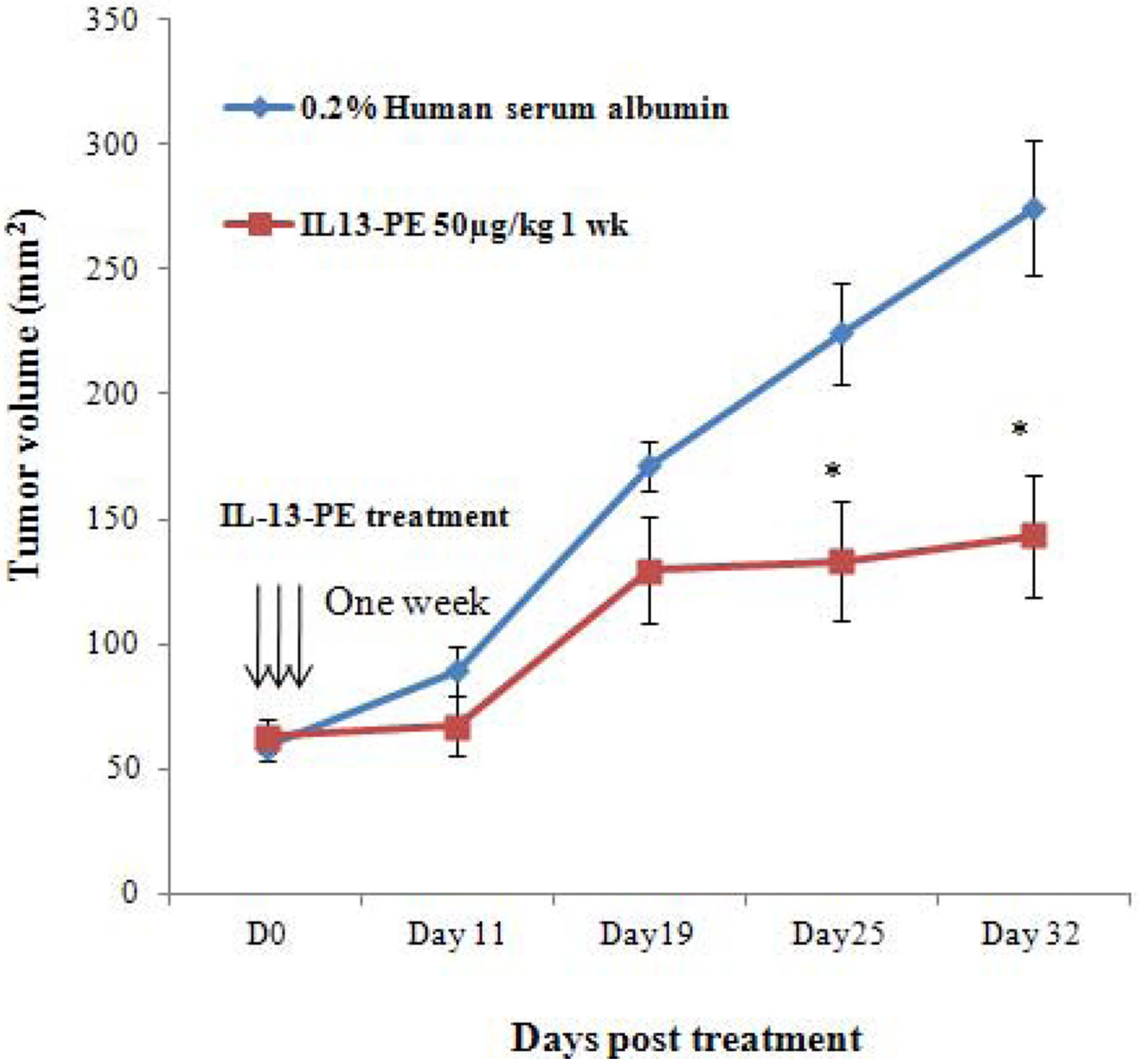

Figure 5.

Intratumoral (IT) and intraperitoneal (IP) IL-13-PE treatment of ACC xenografts significantly reduced tumor growth. **A**) Graph representing the comparison of tumor growth between vehicle and IL-13-PE IT treatment groups (100 µg/kg once a day for one and two weeks indicated by vertical arrows). **B**) Graph representing the comparison of tumor growth between vehicle group and IL-13-PE intraperitoneal treatment group (50 µg/kg; twice a day for a week). Each point represents the mean ± standard error of mean (SEM) from 6 mice in two independent experiments. Statistically significant values are indicated by an asterisk (*$p<0.05$; **$p<0.01$). **C)** Tumor regression in mice with ACC xenograft after treatment with IL-13-PE. (**1–4**) Representative H&E images from IT (**1–2**) and IP (**3–4**) vehicle group (0.2% human serum albumin) with presence of viable tumor cells. (**4–8**) Images represent H&E stained sections from IT (100 µg/kg; **5–6**) and IP (50 µg/kg; **7–8**) treated mice with

IL-13-PE and demonstrates presence of few viable cells with necrotic mass. Images are represented at 2.5X and 20X magnifications.